



## Two-Center Interferences in Dielectronic Transitions in $\text{H}_2^+ + \text{He}$ Collisions

S. F. Zhang,<sup>1,2,\*</sup> D. Fischer,<sup>2</sup> M. Schulz,<sup>2,3</sup> A. B. Voitkiv,<sup>2</sup> A. Senftleben,<sup>2</sup> A. Dorn,<sup>2</sup> J. Ullrich,<sup>2,4</sup>  
X. Ma,<sup>1</sup> and R. Moshhammer<sup>2</sup>

<sup>1</sup>*Institute of Modern Physics, Chinese Academy of Sciences, 730000 Lanzhou, China*

<sup>2</sup>*Max-Planck-Institute for Nuclear Physics, Saupfercheckweg 1, D-69117 Heidelberg, Germany*

<sup>3</sup>*Physics Department and LAMOR, Missouri University of Science and Technology, Rolla, Missouri 65409, USA*

<sup>4</sup>*Physikalisch-Technische Bundesanstalt, Bundesallee 100, D-38116, Braunschweig, Germany*

(Received 29 September 2013; published 13 January 2014)

Molecular two-center interferences in a collision induced excitation of  $\text{H}_2^+$  projectile ions, with simultaneous ionization of helium target atoms, are investigated in a kinematically complete experiment. In the process under investigation, the helium atom is singly ionized and simultaneously the molecular hydrogen ion is dissociated. Different collision mechanisms are identified and interference fringes emerging from a correlated first-order mechanism and from an independent second-order process are observed.

DOI: 10.1103/PhysRevLett.112.023201

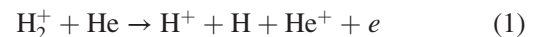
PACS numbers: 34.10.+x, 03.75.-b, 34.50.Fa

Young's double-slit interference is a clear manifestation of the wave character of light. The feasibility of an atomic version of Young's double slit experiment for matter waves in ion-atom collisions was first discussed theoretically by Tuan and Gerjuoy in 1960 [1]. They studied capture processes in collisions of protons with  $\text{H}_2$  and suggested that diffraction of the protons from the two atomic centers of the molecule could lead to interference effects. Only recently, the predictions of Tuan and Gerjuoy were confirmed by several experiments. Variations of the capture cross sections as a function of the molecular orientation could be attributed to interference effects [2–5]. Later, Schmidt *et al.* [6] observed very pronounced matter wave interference fringes in multiple differential momentum spectra of recoil ions produced in dissociative capture in  $\text{H}_2^+ + \text{He}$  collisions.

Such interference effects are more difficult to observe in ionization processes [7], since there the final state of the collision involves at least three unbound particles, as opposed to only two in a capture process (before the subsequent fragmentation of the molecule). The phase angle between the amplitudes associated to the two molecular centers is generally accessible through both the momentum information of the collision and the molecular orientation. Data for ionization in which the phase angle was completely determined are only available for electron impact [8]. For ion impact, interference in projectile diffraction has been observed for fixed projectile energy losses in the scattering angle dependence [9,10]. Interference structures have also been studied in double differential energy distributions of the ejected electrons for fixed emission angles (see, e.g., [11–17]). In all these experiments, the averaging over the phase angles resulted in a damping of the interference patterns, but did not completely eliminate it.

Two-center interference should also occur in the ion-impact induced excitation of a molecule. However, the

experimental observation of this process is particularly challenging because the determination of the phase angle in excitation processes is not straightforward. In this Letter, we present a study of that process using an indirect approach by investigating simultaneous excitation of  $\text{H}_2^+$  projectile ions, resulting in dissociation, and target ionization, in collision with He, i.e.,



in a kinematically complete experiment providing the full phase information. We observe interference structures due to scattering of helium matter waves (in the rest frame of the molecular projectile) from the two atomic centers in the  $\text{H}_2^+$  ions. Two different interaction channels were identified, the first one is based on the electron-electron interaction, and the second one involves two independent electron-nuclear interactions. For this two-electron process, the molecule can be viewed as a double slit in two different ways, which are reflected by different interference patterns depending on which of these two channels is selected: in the first case, the double slit is represented by the two-center electronic wave function and in the second case by the additional two nuclei of the molecule.

The experiment was carried out at the van de Graaff accelerator of the Max Planck Institute for Nuclear Physics in Heidelberg. A beam of 1 MeV  $\text{H}_2^+$  molecular ions was intersected with a supersonic helium gas jet with a temperature of less than 2 K. The momenta of the recoiling helium ions and the ejected low-energy electrons were measured with a conventional reaction microscope [18]. The  $\text{H}^+$  and  $\text{H}^0$  fragments of the dissociated projectile molecular ions were separated by a dipole magnet behind the Reaction Microscope and detected in coincidence with the target particles with two position sensitive detectors about 5 meters behind the reaction region. The longitudinal and transverse

momenta (with respect to the beam axis) of the molecular fragments in their center-of-mass frame are determined by the time-of-flight difference and the positions on the detectors, respectively.

For this beam energy, a momentum resolution for the projectile fragments of about 2 a.u. was achieved. Because of the fact that the typical rotational period of the molecular axis is about 1.5 orders of magnitude larger than the typical dissociation time, the molecular orientation at the instant of the collision can be approximately represented by the momentum vectors of the fragments [19]. Considering the momentum resolution as well as the uncertainty due to rotational excitation of the projectiles, an angular uncertainty for the molecular axis of less than 20 degree is estimated [20].

In the collisions, the molecular ions are excited from the initial  $1s\sigma_g$  state to the final dissociative states, at which the potential energy is converted to a certain kinetic energy release (KER) (see Fig. 1). If only one potential curve is populated, each KER corresponds classically to a specific internuclear distance (neglecting the vibrational energy). For this collision system, excitation to the  $2p\sigma_u$  state is the dominant channel because the required relatively low energy transfer is favored in ion-atom collisions (see [22] and references therein). Using the potential curve of the  $2p\sigma_u$  state, molecular internuclear distance distributions [Fig. 1(c)] are finally calculated from the measured KER distributions.

The reaction channel we studied here is a two-electron transition process. According to perturbation theory, two mechanisms are expected to significantly contribute to this process [23–26]: the first mechanism appears already in first order perturbation theory in the projectile-target interaction proceeding through the electron-electron interaction, which causes a simultaneous transition of both involved electrons. In the following, we refer to this channel as the correlated first-order process ( $ee$ ). In the second mechanism, which

follows from second order perturbation theory, the ionization of the target is caused by an interaction of the  $H_2^+$  core with the target electron and the excitation of the molecule by an independent interaction of the target core with the projectile electron. This channel we call the uncorrelated second-order processes ( $eN$ ).

Using a linear combination of atomic orbitals to approximate the molecular states, the fourfold differential cross section for the correlated first-order process is given by

$$\frac{d^4\sigma_{ee}}{d\theta dq_x dq_y} = \sigma_A^{ee}(\vec{q}) \sin^2(\vec{q} \cdot \vec{Q}/2), \quad (2)$$

here, the cross section is presented using a coordinate system defined by the projectile beam axis, marking the  $z$  direction, and the molecular orientation, marking the  $x$  direction [see Fig. 3(d)],  $\vec{Q}$  is the internuclear vector of the molecule,  $\theta$  is the angle between the internuclear vector and the projectile direction,  $q_x$  and  $q_y$  are the two transverse components of the momentum transfer  $\vec{q}$ , and  $\sigma_A^{ee}(\vec{q})$  is the ionization cross section of helium by a hydrogen atom, differential in  $\vec{q}$ .

With this definition, the geometries of the molecular ions are characterized by only two parameters,  $\theta$  and  $\rho$ , respectively. Two-center interference effects represented by the sinusoidal factor in Eq. (2) will only be observed as a function of the  $x$  component of the momentum transfer.

Because the projectile molecule undergoes a dipole transition during the collision changing its parity from *gerade* to *ungerade*, the cross section must vanish for  $\vec{q} \perp \vec{Q}$  and the oscillations in  $\vec{q} \cdot \vec{Q}$  are phase shifted by  $\pi$  compared to the classical Young-type double-slit interference. Accordingly, the interference in Eq. (2), which represents the target electron behavior, is of a sinusoidal form rather than the general cosinusoidal form.

In the uncorrelated second-order process the two-center nature of the molecular potential affects both the transition in the molecule and the ionization of the target. As far as the molecular transition is concerned, the target nucleus can interact with the molecular electron when it is close to either of the protons, which is not distinguishable. As far as the target ionization is concerned the ejected target electron can get diffracted (in the molecular rest frame) from either of the two protons, which is not distinguishable either. Therefore, each of the two electronic transitions could potentially lead to interference structures. However, due to the abovementioned parity considerations one expects a difference of  $\pi$  of the relative phases of the interfering amplitudes for the two centers. In the case of the transition in the molecule, the symmetry change of the molecular state results in a  $\sin^2$  form of the interference term. In contrast, the ejection of the target electron is not affected by the symmetry of the molecule so that here no phase shift occurs in the corresponding amplitude resulting in a  $\cos^2$  form of the interference term.

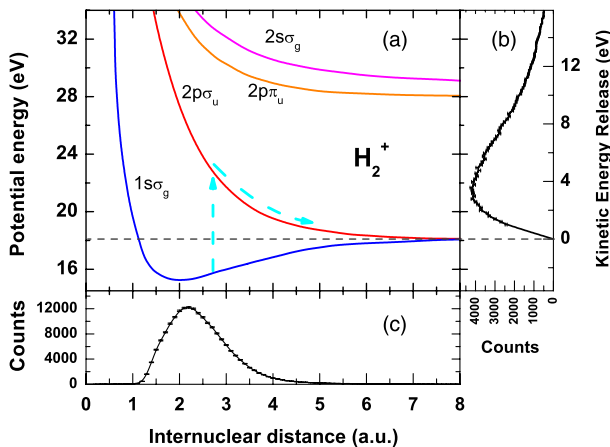


FIG. 1 (color online). (a) Molecular potential curves of  $H_2^+$ , taken from Ref. [21]. (b) Experimental kinetic energy release (KER). (c) Internuclear distance distributions calculated from the KER, assuming that only the  $2p\sigma_u$  state is populated.

Introducing the momentum transferred between the target nucleus and the molecular electron  $\vec{q}_m$  during the transition of the molecular electron and the momentum transferred between the molecular core and the target electron  $\vec{q}_a$  during the ionization of the target, the fourfold differential cross sections can be expressed as a convolution of both transitions. This convolution can be presented differentially in  $\vec{q}_a$  or in  $\vec{q}_m$ . Neglecting initial momenta of the target  $\vec{q}_a \approx \vec{p}_{el}$  and  $\vec{q}_m \approx \vec{p}_{rec}$  yields  $\vec{p}_{el}$  and  $\vec{p}_{rec}$  dependencies of the uncorrelated process, where  $\vec{p}_{rec}$  and  $\vec{p}_{el}$  are the recoil ion momentum and the electron momentum, respectively. For the recoil ion we obtain

$$\frac{d^4\sigma_{eN}}{d\theta dq dp_{rec,x} dp_{rec,y}} \approx \sigma_{A_1}^{eN}(\vec{p}_{rec}) \sin^2(\vec{p}_{rec} \cdot \vec{q}/2) \quad (3)$$

with  $\sigma_{A_1}^{eN}(\vec{p}_{rec}) = \int \sigma_A^{eN}(\vec{p}_{el}, \vec{p}_{rec}) \cos^2(\vec{p}_{el} \cdot \vec{q}/2) d\vec{p}_{el}$ , where  $\sigma_A^{eN}(\vec{p}_{el}, \vec{p}_{rec})$  is the ionization cross section of helium by a hydrogen atom, differential in  $\vec{p}_{el}$  and  $\vec{p}_{rec}$ . Meanwhile, for the electron,

$$\frac{d^4\sigma_{eN}}{d\theta dq dp_{el,x} dp_{el,y}} \approx \sigma_{A_2}^{eN}(\vec{p}_{el}) \cos^2(\vec{p}_{el} \cdot \vec{q}/2) \quad (4)$$

with  $\sigma_{A_2}^{eN}(\vec{p}_{el}) = \int \sigma_A^{eN}(\vec{p}_{el}, \vec{p}_{rec}) \sin^2(\vec{p}_{rec} \cdot \vec{q}/2) d\vec{p}_{rec}$ .

Comparing Eqs. (2), (3), and (4) suggests that the  $\vec{q}$  dependence of the cross sections for the correlated first-order process should exhibit the same interference pattern as the  $\vec{p}_{rec}$  dependence of the cross sections for the uncorrelated second order process. In contrast, the interference pattern in the  $\vec{p}_{el}$  dependence of the cross sections should be phase-shifted by  $\pi$  relative to the former two cross sections. Of course, we cannot test these predictions directly by our data because we cannot distinguish which reaction channel leads to the final state (a fragmented molecule and an ionized target). However, as will be discussed below, we can select kinematic conditions for which some of these mechanisms are approximately separated.

To isolate the first-order correlated mechanism from the second-order uncorrelated process we follow the same approach as was used by Kollmus *et al.* [25] separating corresponding mechanisms leading to simultaneous electron ejection from both collision partners in ion-atom collisions. In the first-order process both the molecular and the atomic cores are essentially passive spectators. Therefore, the total electron momentum ( $p_{el}$ ) should be, on average, significantly larger than the total recoil-ion momentum ( $p_{rec}$ ). Likewise, for the uncorrelated process the target nucleus undergoes a hard interaction with the molecular electron and the recoil-ion momentum should be relatively large. We therefore analyzed fourfold differential cross sections with the additional condition  $p_{el} > 2p_{rec}$  in order to favor the correlated process and with the additional condition  $p_{rec} > 2p_{el}$  in order to favor the uncorrelated process [27].

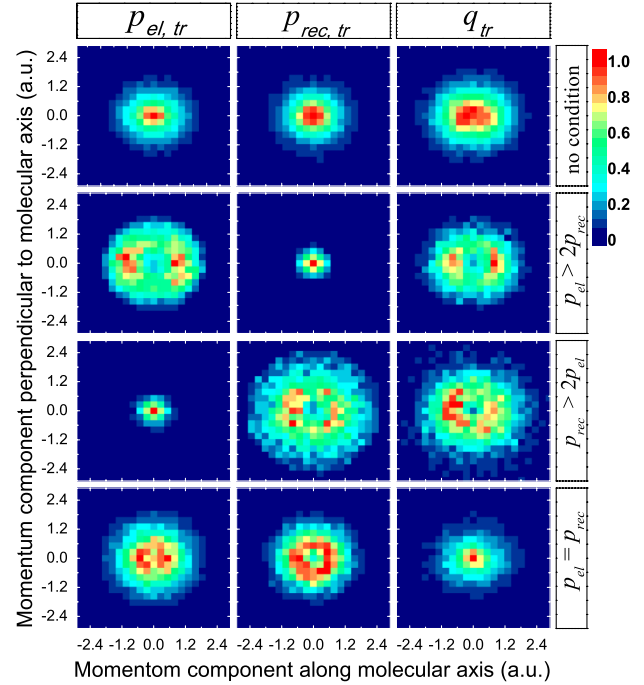


FIG. 2 (color online). Two-dimensional momentum distributions in the  $xy$  plane of the molecular frame. Columns from left to right: electron momentum ( $p_{el,tr}$ ), recoil-ion momentum ( $p_{rec,tr}$ ), and momentum transferred from the molecular ion to the target atom ( $q_{tr}$ ). No indication of interferences was observed when no additional condition was applied. For  $p_{el} > 2p_{rec}$ , interferences in both the electron and the momentum transfer spectra were observed, whereas for  $p_{rec} > 2p_{el}$ , interferences in both the recoil and the momentum transfer spectra were observed. When  $p_{el} = p_{rec}$  (i.e.,  $0.9p_{rec} \leq p_{el} \leq 1.1p_{rec}$ ), no clear indication for interference effect can be found.

In Fig. 2 the measured fourfold differential cross sections are shown as a function of the  $x$  and  $y$  components of the ejected electron momentum, of the recoil momentum, and of the total momentum transferred from the molecular ion to the target atom. According to Eq. (2), a minimum in the correlated cross section would appear at the position of  $p_x = 0$ , regardless of the  $\varphi$  and  $p_y$  values. However, no indication of such a structure was observed in any of the momentum spectra generated without condition on the relation between the electron and recoil-ion momenta. However, with the constraint  $p_{el} > 2p_{rec}$ , a pronounced minimum along a vertical line for  $p_x = 0$  is seen both in the electron momentum spectrum and in the momentum transfer spectrum, while in the recoil-ion momentum spectrum only a sharp maximum at  $p_x = p_y = 0$  is observed. These features are consistent with the interference pattern that is expected for the correlated first-order process.

For the condition  $p_{rec} > 2p_{el}$  (third row) minima along the line for  $p_x = 0$  are found in the recoil-ion momentum and momentum transfer spectra, while this time the electron momentum spectrum exhibits a sharp maximum at  $p_x = p_y = 0$ . This is consistent with the expected pattern

for the uncorrelated second-order mechanism for small electron momenta. However, the interference structure is significantly less pronounced than the one observed in the electron momentum and momentum transfer spectra for the condition  $p_{el} > 2p_{rec}$ . A possible explanation is that the condition  $p_{rec} > 2p_{el}$  not only favors the uncorrelated second-order process, but also other higher-order contributions. For example, higher-order processes involving the scattering of the He core on the molecule nuclei ( $NN$  interaction) could also lead to relatively large recoil-ion momenta and could therefore strongly contribute to the spectra for the condition  $p_{rec} > 2p_{el}$ . This, in turn, could significantly “smear out” the interference pattern.

The spectra for the condition  $p_{rec} = p_{el}$  (fourth row of Fig. 2) are likely to contain significant contributions from both the correlated first-order and the uncorrelated second-order process (as well as other higher-order mechanisms). In these spectra, no clear indication for interference effect can be found. Although there is a pronounced minimum in the recoil-ion momentum spectrum at  $p_x = p_y = 0$ , this cannot be interpreted in terms of two-center interference because, as mentioned above, any interference minimum should occur at  $p_x = 0$  for all values of  $p_y$ . The momentum transfer spectrum exhibits a sharp maximum at the origin; i.e., the momenta are well balanced between the electron and the recoil ion corresponding to dipolelike transitions similar to photoionization.

The absence of interference in the momentum transfer spectrum is not surprising, because the observed distribution is significantly more narrow for the condition  $p_{rec} = p_{el}$  than in the two other cases, and therefore, any oscillation along the  $p_x$  axis could hardly be observed. Moreover, only the correlated first order process should result in such a minimum at  $p_x = 0$ . According to Eqs. (3) and (4), in the uncorrelated second order process a certain value of  $\vec{q}$  does not correspond to a specific value of  $\vec{p}_{rec}$  and  $\vec{p}_{el}$  under the restriction of  $p_{rec} = p_{el}$ , resulting in the blurring of interference structures in  $\vec{q}$ .

The dependence of the observed structures on the internuclear distance  $\varrho$  of the molecular ion can be tested using the reflection approximation (e.g., Ref. [28]). In principle, this could be achieved by applying the abovementioned conditions  $p_{el} > 2p_{rec}$  and  $p_{rec} > 2p_{el}$  and further discriminating the data to specific KERs. However, the conditions used in Fig. 2 are rather restrictive and any additional differentiation of the cross sections results in a very low statistical quality of the spectra that does not easily allow for conclusive statements. Therefore, we chose the less restrictive condition  $|\phi_e - \phi_r| < 120^\circ$  [see Fig. 3(d)], where  $\phi_e$  and  $\phi_r$  are the azimuthal angles of the target electron and the recoil ion, respectively. Here again, the cross sections are likely to contain contributions from all possible mechanisms, i.e., the correlated first-order, the uncorrelated second-order process, as well as other higher-order mechanisms. However, in contrast to the previously discussed

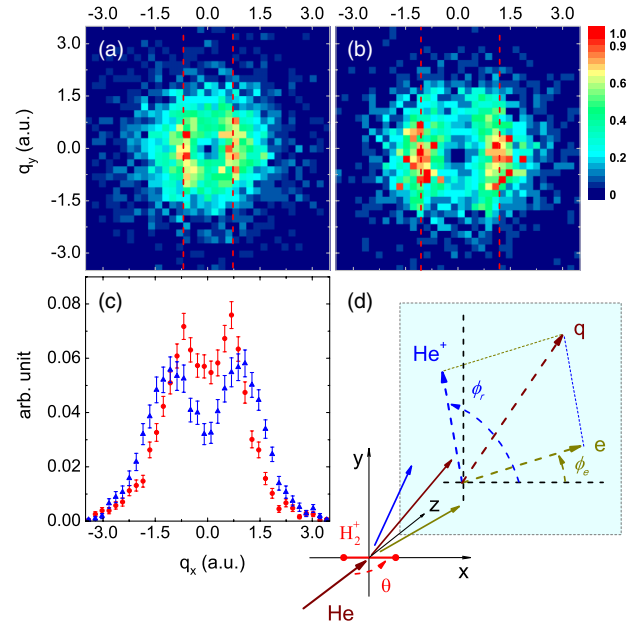


FIG. 3 (color online). Two-dimensional momentum transfer distributions in the transverse plane under different conditions of internuclear distances. Molecular axis perpendicular to the beam direction: (a) KER < 2.5 eV; (b) KER > 8 eV; (c) their  $q_x$  distributions: filled circle for (a), and filled upward triangle for (b). (d) Sketch of the molecular frame and corresponding definitions.

case with  $p_{el} = p_{rec}$ , dipolelike transitions are suppressed and the momentum transfer distribution is substantially broader than the separation between the two expected interference maxima.

In Fig. 3 the projections of the momentum transfer distributions on the azimuthal plane are shown for  $|\phi_e - \phi_r| < 120^\circ$ . Different internuclear distances of the molecular ion were chosen by selecting KERs smaller than 2.5 eV in Fig. 3(a) and larger than 8 eV in Fig. 3(b) corresponding to internuclear distances of  $\varrho \geq 3.2$  a.u. and  $\varrho \leq 2$  a.u. approximately (see Fig. 1). In Fig. 3(c) these cross sections are integrated over the  $y$  direction of the momentum transfer. For both KERs a clear minimum at  $p_x = 0$  is observed and this minimum gets broader with increasing KER corresponding to decreasing  $\varrho$ . Qualitatively, this is in accordance with our simple model; however, the positions of the maxima are at slightly smaller values of  $p_x$  than expected from Eqs. (2) and (3). This might be explained considering the steep dropping of the atomic cross section  $\sigma_A$  with  $\vec{q}$ .

In conclusion, we have investigated simultaneous dissociation and target ionization in collisions between  $H_2^+$  molecular ions and helium atoms in a kinematically complete experiment. We have observed a dependence of the differential cross sections on the orientation of the projectile molecular ion. Compared to earlier studies on Young-type interference in atomic collisions, the present collision system features more degrees of freedom, because

it represents an effective five-body system, consisting of the two active electrons, the two protons in the molecule, and the  $\text{He}^+$  core. In the perturbative description, different first- and higher-order terms contribute to the cross section, a correlated first-order mechanism, and an independent higher-order process. This results in a blurring of oscillating patterns in the integrated cross sections. However, in spite of this rather complex collision system, the two contributing mechanisms can be separated by choosing appropriate kinematic conditions revealing clear interference structures. The observed features agree well with the predictions of two center interference effects in first and second order perturbation theory.

The authors thank Claus Dieter Schröter for careful reading of the manuscript. S. F. Z. and X. M. are supported by the Major State Basic Research Development Program of China (973 Program, Grant No. 2010CB832902) and by the National Nature Science Foundation of China under Grants No. 10979007 and No. 10704076. S. F. Z. is grateful to the CAS-MPS doctor training program. M. S. acknowledges support from the National Science Foundation under Grant No. 0969299.

\*Corresponding author.

zhangshf@impcas.ac.cn

- [1] T. F. Tuan and E. Gerjuoy, *Phys. Rev.* **117**, 756 (1960).
- [2] S. Cheng, C. L. Cocke, V. Frohne, E. Y. Kamber, J. H. McGuire, and Y. Wang, *Phys. Rev. A* **47**, 3923 (1993).
- [3] I. Reiser, C. L. Cocke, and H. Bräuning, *Phys. Rev. A* **67**, 062718 (2003).
- [4] D. Misra, H. T. Schmidt, M. Gudmundsson, D. Fischer, N. Haag, H. A. B. Johansson, A. Källberg, B. Najjari, P. Reinhed, R. Schuch, M. Schöffler, A. Simonsson, A. B. Voitkiv, and H. Cederquist, *Phys. Rev. Lett.* **102**, 153201 (2009).
- [5] H. T. Schmidt, D. Fischer, Z. Berenyi, C. L. Cocke, M. Gudmundsson, N. Haag, H. A. B. Johansson, A. Källberg, S. B. Levin, P. Reinhed, U. Sassenberg, R. Schuch, A. Simonsson, K. Stöckel, and H. Cederquist, *Phys. Rev. Lett.* **101**, 083201 (2008).
- [6] L. P. H. Schmidt, S. Schössler, F. Afaneh, M. Schöffler, K. E. Stiebing, H. Schmidt-Böcking, and R. Dörner, *Phys. Rev. Lett.* **101**, 173202 (2008).
- [7] A. L. Landers, E. Wells, T. Osipov, K. D. Carnes, A. S. Alnaser, J. A. Tanis, J. H. McGuire, I. Ben-Itzhak, and C. L. Cocke, *Phys. Rev. A* **70**, 042702 (2004).
- [8] A. Senftleben, T. Pflüger, X. Ren, O. Al-Hagan, B. Najjari, D. Madison, A. Dorn, and J. Ullrich, *J. Phys. B* **43**, 081002 (2010).
- [9] J. S. Alexander, A. C. Laforge, A. Hasan, Z. S. Machavariani, M. F. Ciappina, R. D. Rivarola, D. H. Madison, and M. Schulz, *Phys. Rev. A* **78**, 060701 (2008).
- [10] K. N. Egodapitiya, S. Sharma, A. Hasan, A. C. Laforge, D. H. Madison, R. Moshhammer, and M. Schulz, *Phys. Rev. Lett.* **106**, 153202 (2011).
- [11] N. Stolterfoht, B. Sulik, V. Hoffmann, B. Skogvall, J. Y. Chesnel, J. Rangama, F. Frémont, D. Hennecart, A. Cassimi, X. Husson, A. L. Landers, J. A. Tanis, M. E. Galassi, and R. D. Rivarola, *Phys. Rev. Lett.* **87**, 023201 (2001).
- [12] S. Chatterjee, D. Misra, A. H. Kelkar, L. C. Tribedi, C. R. Stia, O. A. Fojón, and R. D. Rivarola, *Phys. Rev. A* **78**, 052701 (2008).
- [13] N. Stolterfoht, B. Sulik, L. Gulyás, B. Skogvall, J. Y. Chesnel, F. Frémont, D. Hennecart, A. Cassimi, L. Adoui, S. Hossain, and J. A. Tanis, *Phys. Rev. A* **67**, 030702 (2003).
- [14] D. Misra, A. Kelkar, U. Kadhane, A. Kumar, L. C. Tribedi, and P. D. Fainstein, *Phys. Rev. A* **74**, 060701 (2006).
- [15] H. D. Cohen and U. Fano, *Phys. Rev.* **150**, 30 (1966).
- [16] M. E. Galassi, R. D. Rivarola, P. D. Fainstein, and N. Stolterfoht, *Phys. Rev. A* **66**, 052705 (2002).
- [17] M. E. Galassi, R. D. Rivarola, and P. D. Fainstein, *Phys. Rev. A* **70**, 032721 (2004).
- [18] J. Ullrich, R. Moshhammer, A. Dorn, R. Dörner, L. P. H. Schmidt, and H. Schmidt-Böcking, *Rep. Prog. Phys.* **66**, 1463 (2003).
- [19] R. N. Zare, *J. Chem. Phys.* **47**, 204 (1967).
- [20] R. M. Wood, Q. Zheng, A. K. Edwards, and M. A. Mangan, *Rev. Sci. Instrum.* **68**, 1382 (1997).
- [21] T. E. Sharp, *Atomic Data* **2**, 119 (1970).
- [22] R. G. Cooks, J. Los, and T. R. Govers, in *Collision Spectroscopy* (Springer, New York, 1978), pp. 321–324.
- [23] E. C. Montenegro, W. S. Melo, W. E. Meyerhof, and A. G. de Pinho, *Phys. Rev. Lett.* **69**, 3033 (1992).
- [24] R. Dörner, V. Mergel, R. Ali, U. Buck, C. L. Cocke, K. Froschauer, O. Jagutzki, S. Lencinas, W. E. Meyerhof, S. Nüttgens, R. E. Olson, H. Schmidt-Böcking, L. Spielberger, K. Tökesi, J. Ullrich, M. Unverzagt, and W. Wu, *Phys. Rev. Lett.* **72**, 3166 (1994).
- [25] H. Kollmus, R. Moshhammer, R. E. Olson, S. Hagmann, M. Schulz, and J. Ullrich, *Phys. Rev. Lett.* **88**, 103202 (2002).
- [26] X. Wang, K. Schneider, A. Kelkar, M. Schulz, B. Najjari, A. B. Voitkiv, M. Gudmundsson, M. Grieser, C. Krantz, M. Lestinsky, A. Wolf, S. Hagmann, R. Moshhammer, J. Ullrich, and D. Fischer, *Phys. Rev. A* **84**, 022707 (2011).
- [27] See Supplemental Material at <http://link.aps.org/supplemental/10.1103/PhysRevLett.112.023201> for two-dimensional distributions of  $p_{\text{el}}-p_{\text{rec}}$  space.
- [28] L. P. H. Schmidt, T. Jahnke, A. Czasch, M. Schöffler, H. Schmidt-Böcking, and R. Dörner, *Phys. Rev. Lett.* **108**, 073202 (2012).